Electronic Supplementary Material (ESI) for Lab on a Chip.
This journal is © The Royal Society of Chemistry 2015

Supplementary Information for

Ship-in-a-bottle femtosecond laser integration of optofluidic microlens arrays with center-pass units enabling coupling-free parallel cell counting with 100% success rate

Dong Wu[1], Li-Gang Niu[2], Si-Zhu Wu[1], Jian Xu[1], Katsumi Midorikawa[1], Koji Sugioka[1]

[1]Laser Technology Laboratory, RIKEN, 2-1 Hirosawa, Wako, Saitama 351-0198, Japan.

[2]State Key Laboratory on Integrated Optoelectronics, College of Electronic Science and Engineering, Jilin University, 2699 Qianjin Street, Changchun, 130012, People's Republic of China.

Correspondence: Professor K Sugioka, Laser Technology Laboratory, RIKEN, 2-1 Hirosawa, Wako, Saitama 351-0198, Japan, TEL: 048-467-9492, FAX: 048-462-4682.

E-mail: ksugioka@riken.jp

Table of Contents

◆ Figures S1 to S9 (pages 2 to 6)

◆ Tables S1 and S2 (pages 7 and 8)

◆ Captions for Supporting Videos 1 and 2 (page 9)

Figure S1. System for characterizing the cell detection by ship-in-a-bottle integrated optofluidic microlenses. It consists of a halogen lamp, CCD, and 20× objective lens. Under illumination from the halogen lamp, the focal spots and images are magnified by the objective lens and collected by the CCD. Solvents containing cells are introduced into the biochip using a pump. When no cell is above the microlens, the intensity is a maximum. The intensity decreases when a cell moves across because the cell scatters, reflects, and absorbs light. Therefore, every intensity dip implies that a cell is passing above the microlens.

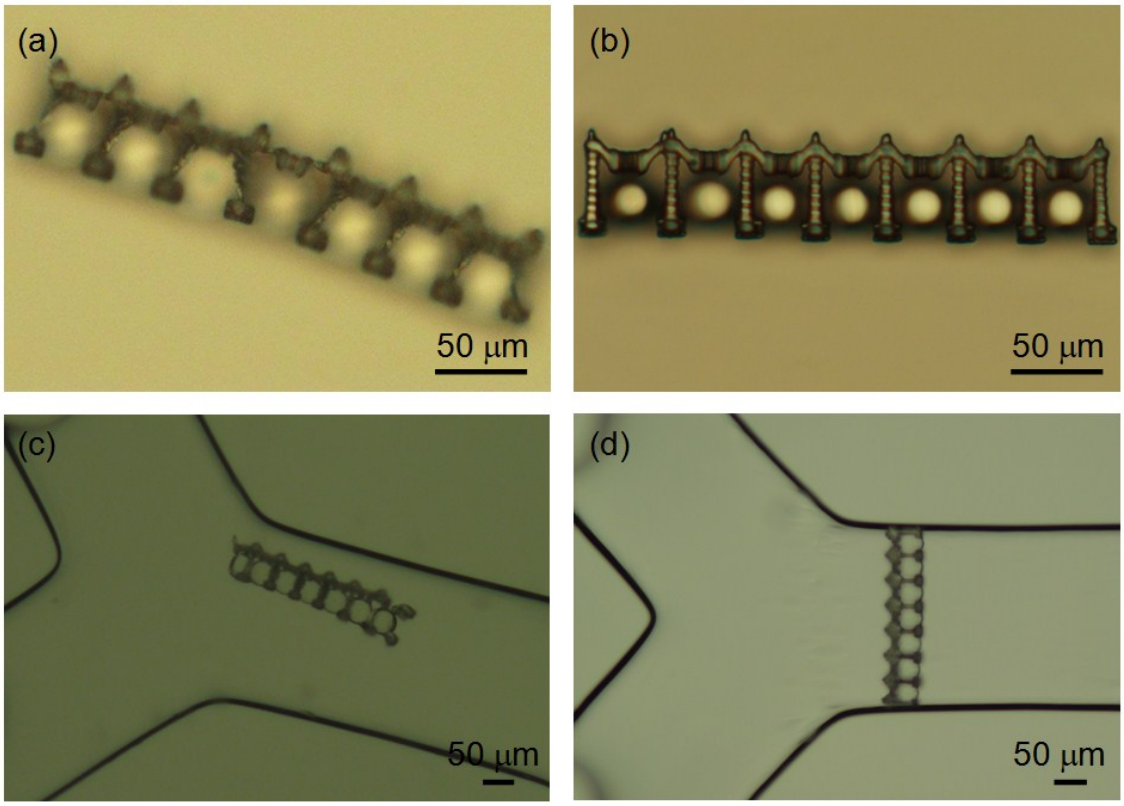

Figure S2. Optimal laser power for fabricating high quality M-shape confining walls. The wall thickness prepared at a normal laser power of 50 μW is 6 μm, as shown in Figs. 3(a) and 3(b). However, such structures easily deform due to the large 40 -μm height of the wall (a). To avoid this deformation, a higher laser power of 70 μW is adopted to produce the thicker wall of 8 μm (b). During the channel fabrication shown in (d), the optimum laser power was increased to 140 μW due to reflection and scattering at the channel/polymer interface as well as multiphoton absorption in the glass and the polymer. In contrast, 100 μW leads to the deformation and collapse evident in (c)]. In addition, 15 μm-wide support pillars were fabricated to keep the device constructed during the solvent development process.

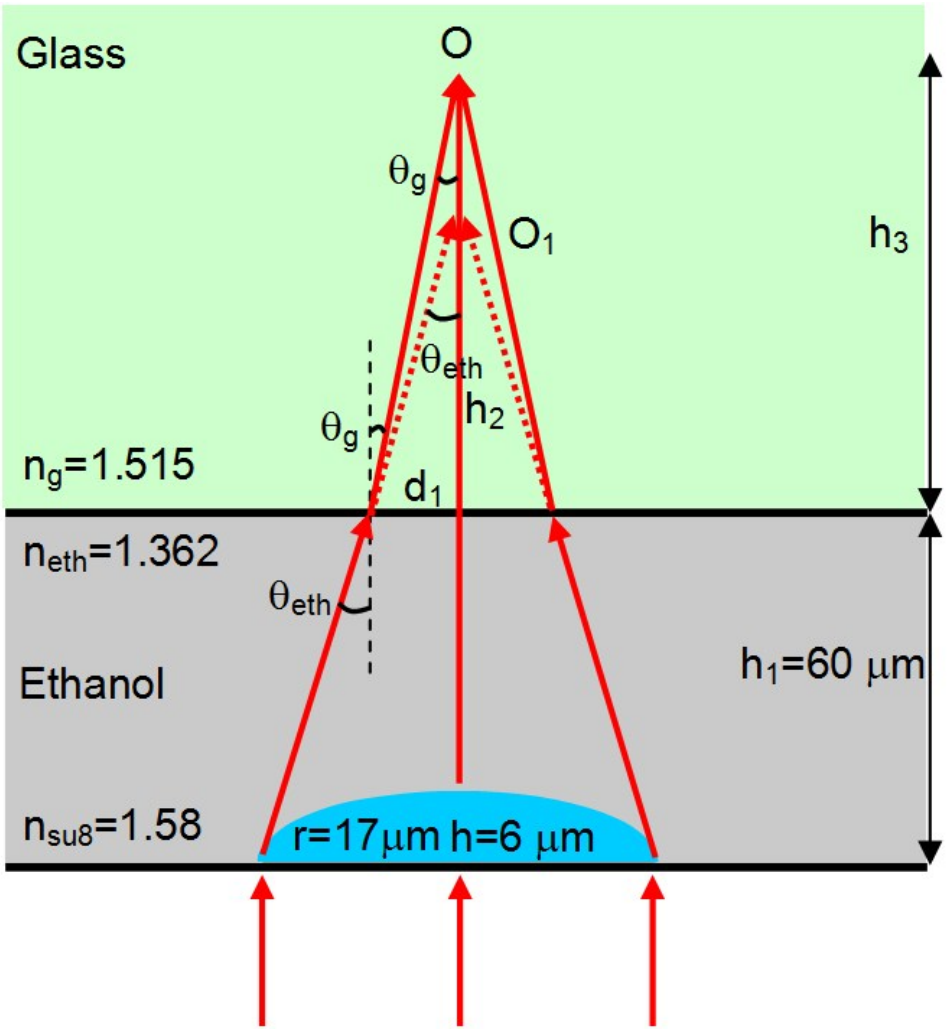

Figure S3. Calculation of the focal length of a microlens in a closed microfluidic channel by the aplanatic principle and refraction theory. The light is focused by the microlens and passes through two different media (ethanol and glass) with refraction at their interface. The original focal spot at position "O_1" is thereby displaced to position "O." Position "O_1" is determined by the aplanatic principle as

$$hn_{su8} + (h_1 - h + h_2)n_{eth} = n_{eth}\sqrt{r^2 + (h_1 + h_2)^2}\ .$$

Given h = 6 μm, h_1 = 60 μm, n_{su8} = 1.58, n_{eth} = 1.362, and r = 17 μm, one finds

$$h_2 = \frac{n_{eth}^2(r^2 + h^2) - h^2 n_{su8}^2}{2hn_{eth}(n_{su8} - n_{eth})} - h_1 + h = 90\ \mu\text{m}$$

and

$$\tan\theta_{\text{eth}} = \frac{r}{h_1 + h_2} = \frac{17}{150} = 0.1133$$

so that

$$\theta_{\text{eth}} = \tan^{-1} 0.1133 = 6.508° .$$

However,

$$d_1 = h_2 \tan\theta_{\text{eth}} = 90 \times 0.1133 = 10.197 \ \mu\text{m}$$

According to refraction theory, $n_{\text{eth}} \sin\theta_{\text{eth}} = n_{\text{g}} \sin\theta_{\text{g}}$, so that

$$\theta_{\text{g}} = \sin^{-1}\left(\frac{n_{\text{eth}}}{n_{\text{g}}} \sin\theta_{\text{eth}} \right) = 5.848°$$

and

$$h_3 = d_1 / \tan\theta_{\text{g}} = 10.197 / \tan 5.848° = 99.55 \ \mu\text{m} .$$

Finally, the focal length $f = h_1 + h_3 = 159.6 \ \mu\text{m}$ is obtained, which agrees with the measured value of 155±5 μm. In air, according to the aplanatic principle,

$$hn_{\text{su8}} + f - h = \sqrt{r^2 + f^2} .$$

Given h = 6 μm, n_{su8} = 1.58, and r = 17 μm, one obtains

$$f = \frac{r^2 + h^2 - h^2 n_{\text{su8}}^2}{2h(n_{\text{su8}} - 1)} + h = 39.8 \ \mu\text{m}$$

which agrees with the measured value of 42±3 μm.

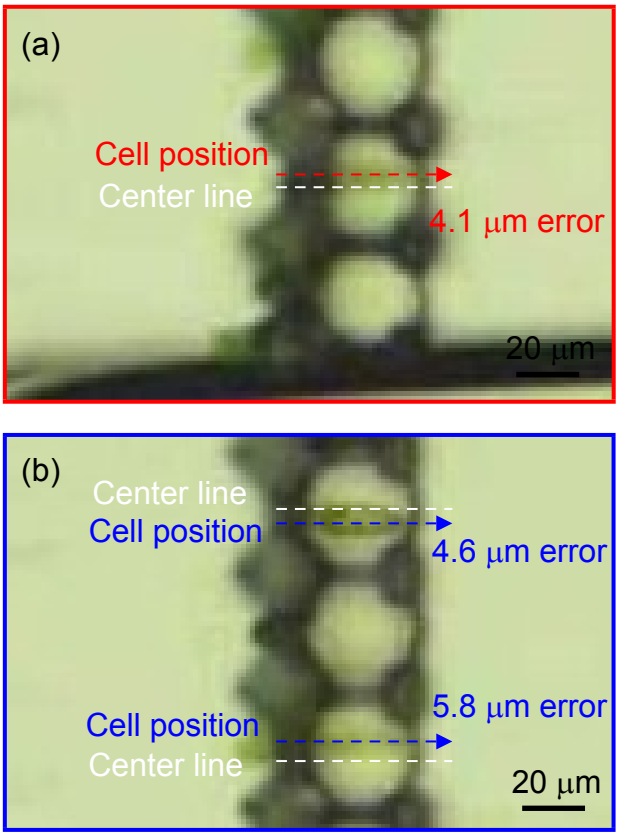

Figure S4. Deviation between the cell position and the center of each microlens. The apertures in the confining wall force most cells to pass above the center of a microlens, but there are some slight variations because the apertures are slightly larger than the cells. Examples of deviations can be seen in these magnified images of Figs. 4(a)–(b). The errors are estimated to be less than ±6 μm.

Lens array	Lens 1	Lens 2	Lens 3	Lens 4	Lens 5	Lens 6	Lens 7
Flat surface	0.984	0.969	0.996	0.984	0.969	0.996	0.992
In channel	0.902	1	0.996	0.996	0.961	0.925	0.902

Table S1. Optical intensities at seven focal spots of a MLA on a flat surface and in a channel. The normalized greyscale intensity of the focal spot array is extracted from the images in Figs. 3(c) and 3(d). The deviation in the intensity on the flat surface is (0.996–0.969)/2 = 1.4% from Fig. 3(e), whereas that in the channel is (1–0.902)/2 = 4.9% from Fig. 3(f). Due to the influence of the channel sidewalls, the optical intensities of the focal spots adjacent to the sidewalls (for lenses 1 and 7) are a little lower than those of the other lenses, which results in a higher deviation.

Lens array	Lens 1	Lens 2	Lens 3	Lens 4	Lens 5	Lens 6	Lens 7
Flat surface (μm)	2.25	2.6	2.06	2.4	2.36	2.08	2.33
In channel (μm)	3.02	3.66	3.66	3.76	3.39	3.52	3.54

Table S2. Full width at half maximum (FWHM) of the normalized optical intensity of the seven focal spots of a MLA on a flat surface and in a channel. The average FWHM of the focal spots of the MLA in air (with $n = 1$) is (2.25+2.6+2.06+2.4+2.36+2.08+2.33)/7 = 2.3 μm, whereas that in the channel filled with ethanol (for which $n = 1.362$) is (3.02+3.66+3.66+3.76+3.39+3.52+3.54)/7 = 3.51 μm. The reason the FWHM in a channel is much bigger than in air is because the focal length of the MLA in a channel is larger than in air, owing to the small difference in the refractive index of the polymer ($n = 1.58$) and of the ethanol ($n = 1.362$).

Supporting Video 1. The center-pass function of an optofluidic device to control the cell position. At the four-second mark in this video, a cell passes through the aperture in the 2nd confining wall. Then, it passed the M-shape structures and the 2nd microlens from right to left. Finally, it reaches the right side of the device. Likewise, at the nine- and ten-second marks, three cells pass above the centers of the 3rd, 5th, and 7th microlenses from right to left.

Supporting Video 2. The filtering function of an M-shaped center-pass optofluidic MLA. Some cells are round due to a biological deformation. The diameter of such deformed cells can be as large as 15 μm, and those cells are hindered by the 9-μm apertures in the confining wall. At the five- and ten-second marks, two deformed cells are hindered by the M-shaped center-pass wall. However, three normal cells with 6–8 μm width freely pass the apertures at the six-, fifteen-, and nineteen-second marks. To clearly observe the resulting filtering, the flow speed of the water is reduced to as low as 80-150 μm/s.